

Supplement of Atmos. Chem. Phys., 18, 16033–16050, 2018
<https://doi.org/10.5194/acp-18-16033-2018-supplement>
© Author(s) 2018. This work is distributed under
the Creative Commons Attribution 4.0 License.



Supplement of

Global streamflow and flood response to stratospheric aerosol geoengineering

Liren Wei et al.

Correspondence to: Duoying Ji (duoyingji@gmail.com) and John C. Moore (john.moore.bnu@gmail.com)

The copyright of individual parts of the supplement might differ from the CC BY 4.0 License.

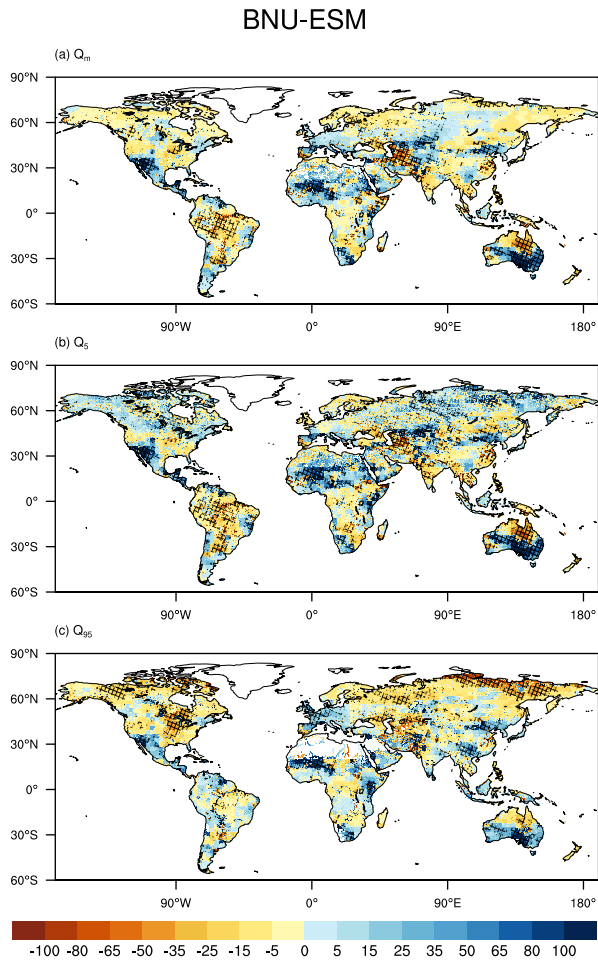


Figure S1: Relative difference of three streamflow indicators between G4 and RCP4.5 during the period of 2030-2069, as percentages of RCP4.5: $(G4-RCP4.5)/RCP4.5 \times 100\%$, projected by BNU-ESM. Top, annual mean flow (Q_m); Middle, annual high flow (Q_5); Bottom, annual low flow (Q_{95}). For each streamflow level, grid cells with less than 0.01 mm/day are masked out. Hashed areas indicate locations where the streamflow changes are significant at the 95% level using the two-sample MW-U test.

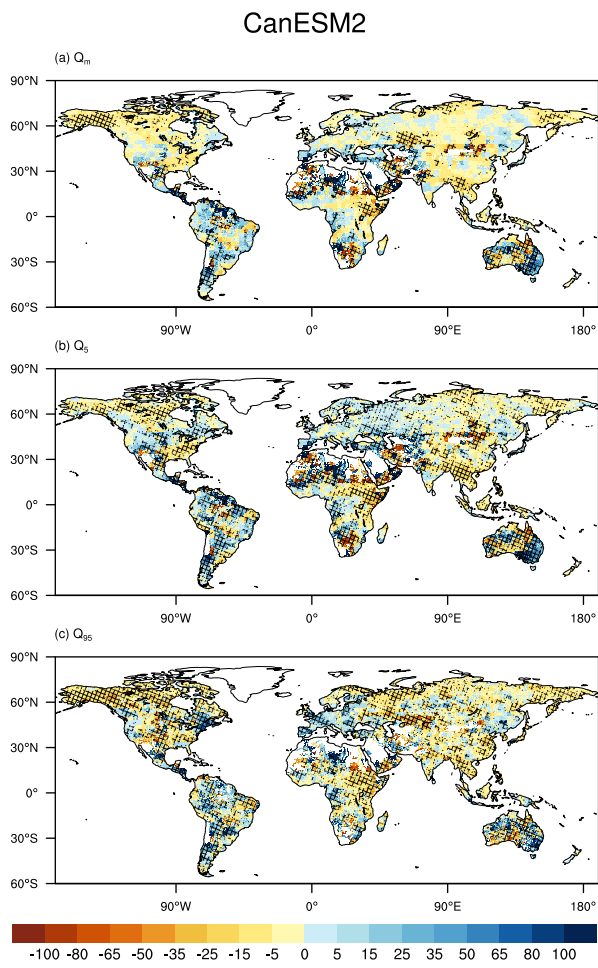


Figure S2: Relative difference of three streamflow indicators between G4 and RCP4.5 during the period of 2030-2069, as percentages of RCP4.5: $(G4-RCP4.5)/RCP4.5 \times 100\%$, projected by CanESM2. Top, annual mean flow (Q_m); Middle, annual high flow (Q_5); Bottom, annual low flow (Q_{95}). For each streamflow level, grid cells with less than 0.01 mm/day are masked out. Hashed areas indicate locations where the streamflow changes are significant at the 95% level using the two-sample MW-U test.

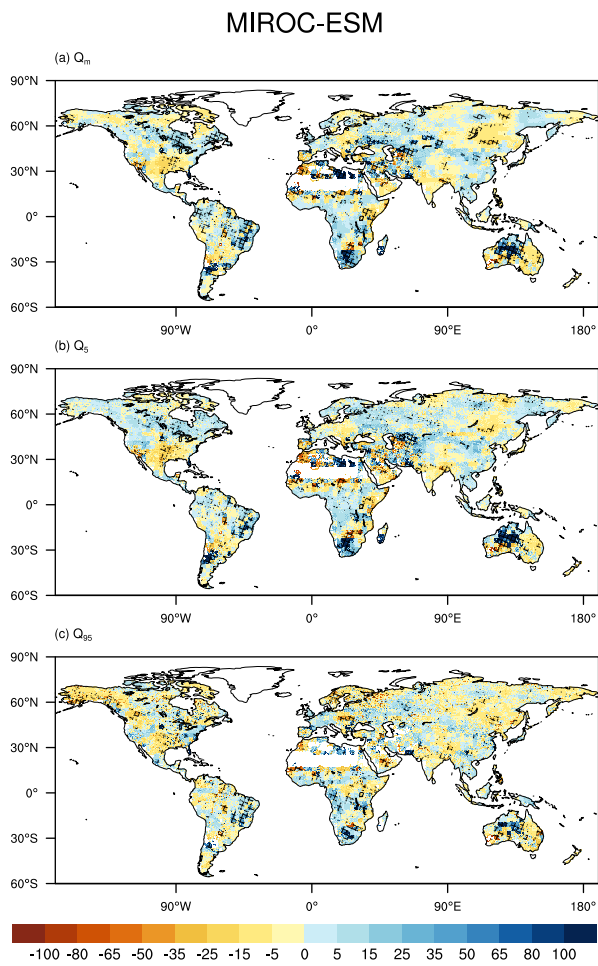


Figure S3: Relative difference of three streamflow indicators between G4 and RCP4.5 during the period of 2030-2069, as percentages of RCP4.5: $(G4-RCP4.5)/RCP4.5 \times 100\%$, projected by MIROC-ESM. Top, annual mean flow (Q_m); Middle, annual high flow (Q_5); Bottom, annual low flow (Q_{95}). For each streamflow level, grid cells with less than 0.01 mm/day are masked out. Hashed areas indicate locations where the streamflow changes are significant at the 95% level using the two-sample MW-U test.

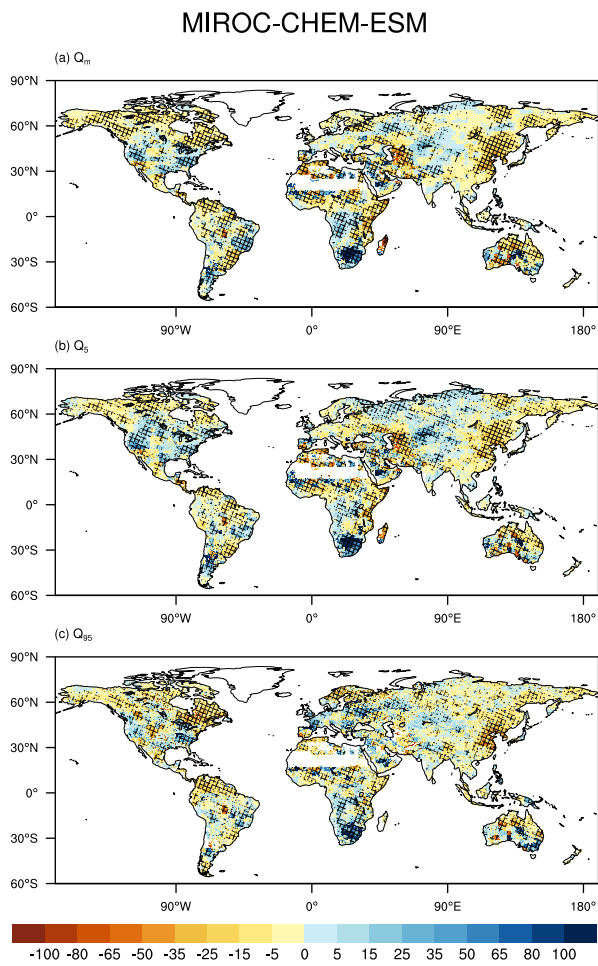


Figure S4: Relative difference of three streamflow indicators between G4 and RCP4.5 during the period of 2030-2069, as percentages of RCP4.5: $(G4-RCP4.5)/RCP4.5 \times 100\%$, projected by MIROC-ESM-CHEM. Top, annual mean flow (Q_m); Middle, annual high flow (Q_5); Bottom, annual low flow (Q_{95}). For each streamflow level, grid cells with less than 0.01 mm/day are masked out. Hashed areas indicate locations where the streamflow changes are significant at the 95% level using the two-sample MW-U test.

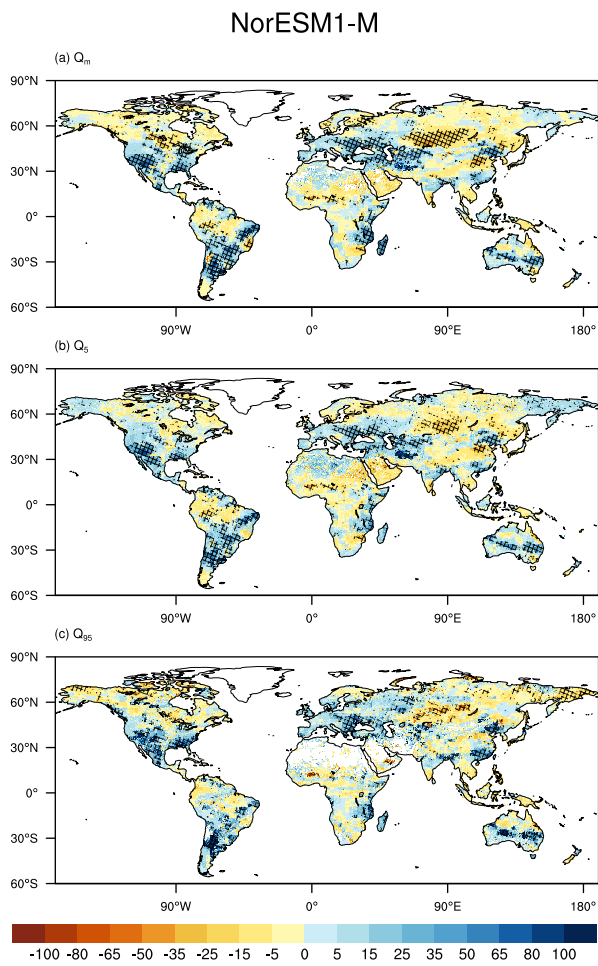


Figure S5: Relative difference of three streamflow indicators between G4 and RCP4.5 during the period of 2030-2069, as percentages of RCP4.5: $(G4-RCP4.5)/RCP4.5 \times 100\%$, projected by NorESM1-M. Top, annual mean flow (Q_m); Middle, annual high flow (Q_5); Bottom, annual low flow (Q_{95}). For each streamflow level, grid cells with less than 0.01 mm/day are masked out. Hashed areas indicate locations where the streamflow changes are significant at the 95% level using the two-sample MW-U test.

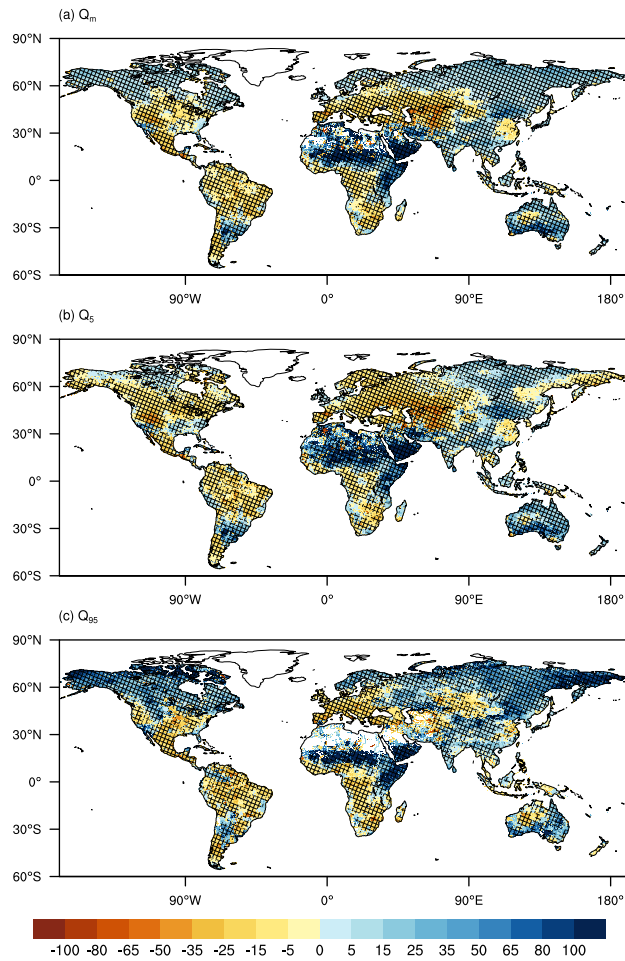


Figure S6: Relative difference of three streamflow indicators between RCP4.5 (2030-2069) and historical (1960-1999), as percentages of historical: (RCP4.5-historical)/historical×100%. Top, annual mean flow (Q_m); Middle, annual high flow (Q_5); Bottom, annual low flow (Q_{95}). For each streamflow level, grid cells with less than 0.01 mm/day are masked out. Hashed areas indicate locations where the streamflow changes are significant at the 95% level using the two-sample MW-U test.

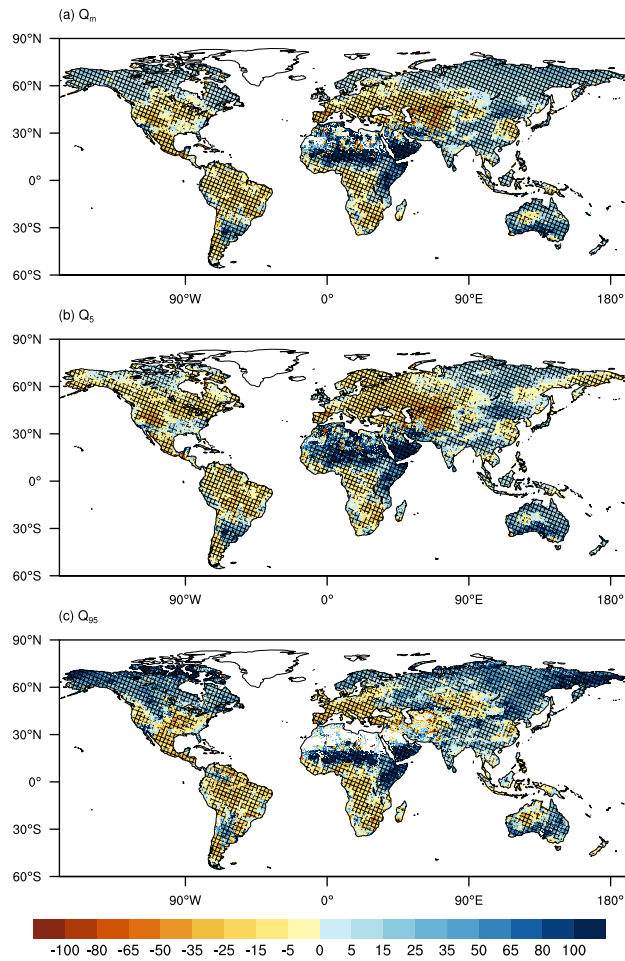


Figure S7: Relative difference of three streamflow indicators between G4 (2030-2069)

and historical (1960-1999), as percentages of historical: $(G4 - \text{historical})/\text{historical} \times 100\%$. Top, annual mean flow (Q_m); Middle, annual high flow (Q_5); Bottom, annual low flow (Q_{95}). For each streamflow level, grid cells with less than 0.01 mm/day are masked out. Hashed areas indicate locations where the streamflow changes are significant at the 95% level using the two-sample MW-U test.

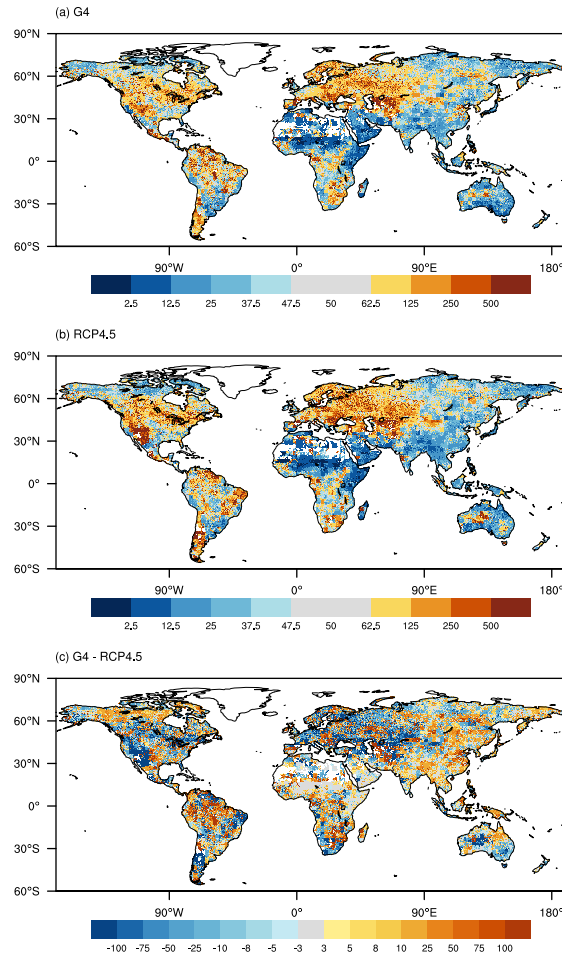


Figure S8: Multi-model ensemble median of return periods for discharge which correspond to 50-year return period level in the historical simulation (1960-1999) under (a) G4, (b) RCP4.5 and (c) the difference of G4 and RCP4.5. Grid cells in extremely dry regions in historical simulation, i.e. $Q_m < 0.01 \text{ mm/day}$ are masked out.

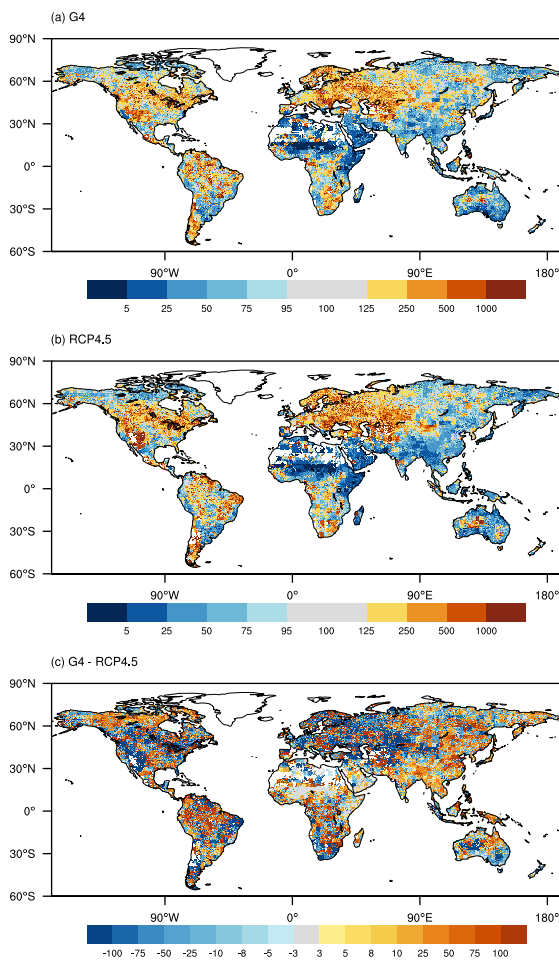


Figure S9: Multi-model ensemble median of return periods for discharge which correspond to 100-year return period level in the historical simulation (1960-1999) under (a) G4, (b) RCP4.5 and (c) the difference of G4 and RCP4.5. Grid cells in extremely dry regions in historical simulation, i.e. $Q_m < 0.01 \text{ mm/day}$ are masked out.

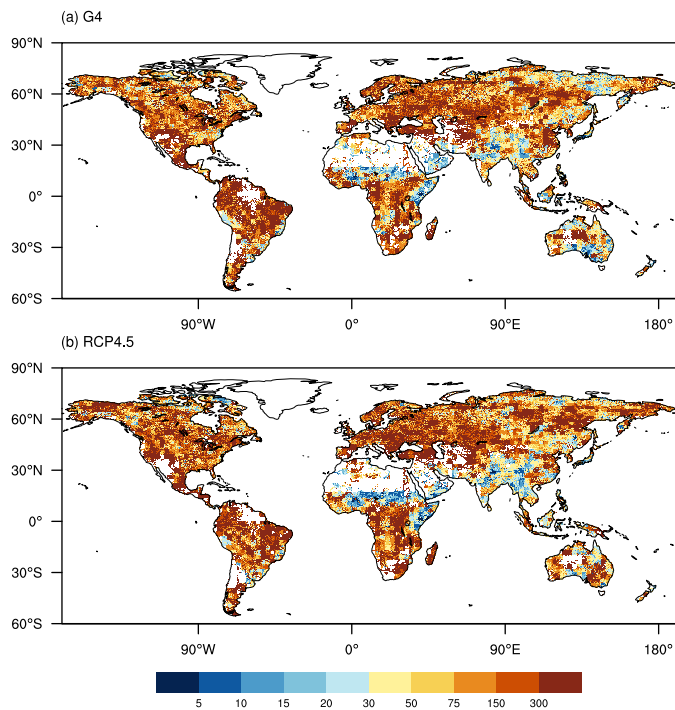


Figure S10: Multi-model ensemble range of return period for discharge that correspond with the 30-year return period in the historical simulation (1960-1999) under (a) G4 and (b) RCP4.5 scenarios, as the difference between maximum and minimum return periods. Grid cells in extremely dry regions, i.e. $Q_m < 0.01$ mm/day and extreme high value of return period regions are masked out.